Inorg. Chem. **2007**, *46*, 7827–7839

Electronic Structures of Tris(dioxolene)chromium and Tris(dithiolene)chromium Complexes of the Electron-Transfer Series $[Cr(dioxolene)_3]^z$ and $[Cr(dithiolene)_3]^z$ ($z = 0, 1-, 2-, 3-$). A Combined Experimental and Density Functional Theoretical Study

Ruta R. Kapre,[†] Eberhard Bothe,[†] Thomas Weyhermüller,[†] Serena DeBeer George,[‡] Nicoleta Muresan,[†] and Karl Wieghardt*[,†]

Max-Planck-Institut für Bioanorganische Chemie, Stiftstrasse 34-36, D-45470 Mülheim an der Ruhr, Germany, and Stanford Synchroton Radiation Laboratory, SLAC, Stanford University, Stanford, California 94309

Received May 4, 2007

From the reaction mixture of 3,6-di-*tert*-butylcatechol, $H_2[^{3,6}L_{cat}]$, $[CrCl_3(thf)_3]$, and NEt_3 in CH_3CN in the presence of air, the neutral complex $[Cr^{III}(^{3,6}L^{\bullet}_{sq})_3]$ ($S = 0$) (**1**) was isolated. Reduction of **1** with $[Co(Cp)_2]$ in CH_2Cl_2 yielded microcrystals of $[Co(Cp)_2][Cr^{III}(^{3,6}L^{\bullet}_{sq})_2(^{3,6}L_{cat})]$ ($S = {}^1/_2$) (**2**) where $(^{3,6}L^{\bullet}_{sq})^{1-}$ is the π-radical monoanionic *o*-semiquinonate of the catecholate dianion $(^{3,6}L_{cat})^{2-}$. Electrochemistry demonstrated that both species are members of the electron-transfer series $[Cr(^{3,6}L_{O,O})]^z$ ($z = 0, 1-, 2-, 3-$). The corresponding tris(benzo-1,2-dithiolato)chromium complex $[N(n\text{-}Bu)_4][Cr^{III}(^{3,5}L^{\bullet}_{S,S})_2(^{3,5}L_{S,S})]$ ($S = {}^1/_2$) (**3**) has also been isolated; $(^{3,5}L_{S,S})^{2-}$ represents the closed-shell dianion 3,5-di-*tert*-butylbenzene-1,2-dithiolate(2–), and $(^{3,5}L^{\bullet}_{S,S})^{1-}$ is its monoanionic π radical. Complex **3** is a member of the electron-transfer series $[Cr(^{3,5}L_{S,S})_3]^z$ ($z = 0, 1-, 2-, 3-$). It is shown by Cr K-edge and S K-edge X-ray absorption, UV–vis, and EPR spectroscopies, as well as X-ray crystallography, of **1** and **3** that the oxidation state of the central Cr ion in each member of both electron-transfer series remains the same (+III) and that all redox processes are ligand-based. These experimental results have been corroborated by broken symmetry density functional theoretical calculations by using the B3LYP functional.

Introduction

It is well established that substituted and unsubstituted catecholates(2−), which are the doubly deprotonated forms of 1,2-dihydroxybenzene derivatives, undergo two successive, reversible one-electron oxidation steps yielding the π-radical, monoanionic *o*-semiquinonates(1−), and neutral *o*-benzoquinones (Scheme 1). The coordination chemistry of all three forms with transition metal ions has been intensively studied, and their chemistry has been comprehensively reviewed.[1] They are considered to be archetypical noninnocent ligands.

Early work by Raymond et al.,[2] Pierpont et al.,[3] and more recently by Kitagawa et al.[4] had established that the electron-transfer series of tris(dioxolene)chromium(III) complexes, where dioxolene represents a benzene-1,2-oxo ligand of unspecified oxidation level (catecholate, *o*-semiquinonate, or benzo-1,2-quinone), consists of at least four members, as in eq 1. These authors have assigned a spectroscopic

$$[Cr^{III}(L^{\bullet}_{sq})_3]^0 \underset{-e}{\overset{+e}{\rightleftharpoons}} [Cr^{III}(L^{\bullet}_{sq})_2(L_{cat})]^{1-} \underset{-e}{\overset{+e}{\rightleftharpoons}} [Cr^{III}(L^{\bullet}_{sq})(L_{cat})_2]^{2-} \underset{-e}{\overset{+e}{\rightleftharpoons}} [Cr^{III}(L_{cat})_3]^{3-} \quad (1)$$

* To whom correspondence should be addressed. E-mail: wieghardt@mpi-muelheim.mpg.de.
[†] Max-Planck-Institut für Bioanorganische Chemie.
[‡] Stanford University.

(1) (a) Pierpont, C. G. *Coord. Chem. Rev.* **2001**, *216−217*, 99. (b) Pierpont, C. G. *Coord. Chem. Rev.* **2001**, *219−221*, 415. (c) Pierpont, C. G.; Lange, C. W. *Progr. Inorg. Chem.* **1994**, *41*, 331. (d) Pierpont, C. G.; Buchanan, R. M. *Coord. Chem. Rev.* **1981**, *38*, 45.

(2) (a) Sofen, S. R.; Ware, D. C.; Cooper, S. R.; Raymond, K. N. *Inorg. Chem.* **1979**, *18*, 234. (b) Raymond, K. N.; Jsied, S. S.; Brown, L. D.; Fronczek, F. R.; Nibert, J. H. *J. Am. Chem. Soc.* **1976**, *98*, 1767. (c) Jsied, S. S.; Kuo, G.; Raymond, K. N. *J. Am. Chem. Soc.* **1976**, *98*, 176.

(3) (a) Pierpont, C. G.; Downs, H. H. *J. Am. Chem. Soc.* **1976**, *98*, 4834. (b) Buchanan, R. M.; Claflin, J.; Pierpont, C. G. *Inorg. Chem.* **1983**, *22*, 2552.

(4) (a) Chang, H.-C.; Myasaka, H.; Kitagawa, S. *Inorg. Chem.* **2001**, *40*, 146. (b) Chang, H.-C.; Kitagawa, S. *Angew. Chem., Int. Ed.* **2002**, *41*, 130.

10.1021/ic7008607 CCC: $37.00
Published on Web 08/23/2007

Scheme 1. Ligands and Complexes

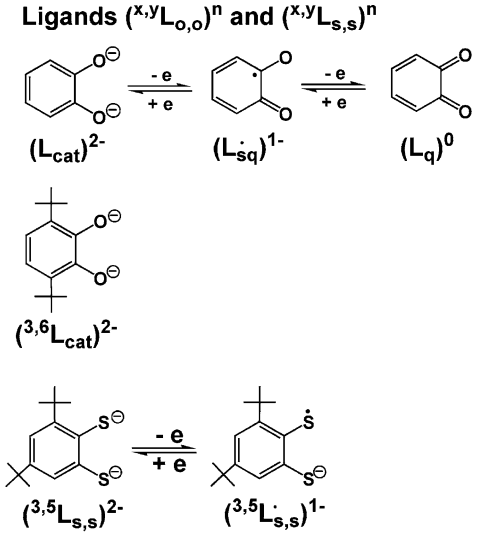

Complexes

$[Cr^{III}(^{3,6}L^{\cdot}_{sq})_3]$	(S = 0)	1
$[Co(Cp)_2][Cr^{III}(^{3,6}L^{\cdot}_{sq})_2(^{3,6}L_{cat})]$	(S = 1/2)	2
$[N(n\text{-}Bu)_4][Cr^{III}(^{3,5}L^{\cdot}_{s,s})_2(^{3,5}L_{s,s})]$	(S = 1/2)	3
$[Cr^{V}O(^{3,5}L_{s,s})_2]$	(S = 1/2)	4

oxidation state of +III (d^3) for the central chromium ion throughout the series. The redox chemistry has then been described as ligand-centered processes. The above charge distribution was bolstered by spectroscopy (electronic absorption, EPR), magnetochemistry, X-ray crystallography, and to a lesser extent, by MO theoretical calculations.

In contrast, since 2001 Lay et al.[5−7] argued in a number of papers that the monoanion, $[Cr(dioxolene)_3]^-$, should be described as Cr(V) species with three closed-shell catecholate(2−) ligands, $[Cr^V(L_{cat})_3]^-$, and similarly, that the dianion, $[Cr(dioxolene)_3]^{2-}$, is a Cr(IV) species containing again three catecholate(2−) ligands, $[Cr^{IV}(L_{cat})_3]^{2-}$. This idea has been refuted by Pierpont.[8] Lay et al.[5−7] have reported the Cr K-edge X-ray absorption spectra of the mono-, di-, and trianion but *not* of the neutral complex $[Cr(dioxolene)_3]$ for which they propose—in agreement with all other authors—that the electronic structure is to be described as $[Cr^{III}(L^{\bullet}_{sq})_3]$ ($S = 0$) without providing X-ray absorption spectra (XAS) data or other additional, new evidence.

Thus, according to Lay et al.,[5−7] the reversible one-electron transfer wave in the cyclic voltammogram between the neutral complex and its monoanion encompasses a dramatic change of the charge distribution at the central Cr ion, namely from Cr(V) in the monoanion to Cr(III) (upon one-electron *oxidation*!) in the neutral species, see eq 2.

$$[Cr^V(L_{cat})_3]^- \overset{-e}{\underset{+e}{\rightleftharpoons}} [Cr^{III}(L^{\bullet}_{sq})_3]^0 \quad (2)$$

Thus, the largest change in energy of the Cr K-edges and pre-edges in the XAS between two one-electron related species of the present electron-transfer series, eq 1, should be observed on going from the monoanion (Cr^V) to the neutral complex (Cr^{III}). Note that a change of ∼1 eV per oxidation number is considered to be a reasonable indication for a change of oxidation state by one unit at the transition metal ion. Here, one might therefore expect a change of ∼2 eV. For example, light-induced oxidation of $[Fe^{III}(cyclam\text{-}ac)(N_3)]^+$ as in eq 3 has been reported to bring about a change of the iron pre-edge energy of 2 eV.[9]

$$[Fe^{III}(cyclam\text{-}ac)N_3]^+ \xrightarrow[-N_2]{h\nu} [Fe^V(N)(cyclam\text{-}ac)]^+ \quad (3)$$

We have synthesized and fully characterized a new neutral species, namely $[Cr^{III}(^{3,6}L^{\bullet}_{sq})_3]$ ($S = 0$) (**1**) and its monoanion in $[Co(Cp)_2][Cr(^{3,6}L_{O,O})_3]$ ($S = {}^1/_2$) (**2**) and measured their UV−vis, EPR, and Cr K-edge XAS data. In addition, we have performed broken symmetry (BS) density functional (DFT) calculations (B3LYP) in order to obtain a consistent picture of the electronic structure of both species.

In order to demonstrate a ligand-centered redox process in eq 2, we also synthesized the 3,5-di-*tert*-butylbenzene-1,2-dithiolate analogue of **2**, namely $[N(n\text{-}Bu)_4][Cr^{III}(^{3,5}L^{\bullet}_{S,S})_2(^{3,5}L_{S,S})]$ ($S = {}^1/_2$) (**3**), and characterized this novel tris(benzene-1,2-dithiolene)chromium monoanionic species by X-ray crystallography. We have recorded the Cr K-edge and the S K-edge spectra of **3**, and we have established that **3** is also a member of a four-membered electron-transfer series $[Cr(^{3,5}L_{S,S})_3]^z$ ($z = 0, 1-, 2-, 3-$) and calculated the electronic structure of each member by using BS DFT methodology.

Experimental Section

The ligand 3,6-di-*tert*-butylcatechol, $H_2[^{3,6}L_{cat}]$, was prepared according to the literature;[10] the ligand 3,5-di-*tert*-butylbenzene-1,2-dithiol, $H_2[^{3,5}L_{S,S}]$, was synthesized as is described in ref 11.

$[Cr^{III}(^{3,6}L^{\bullet}_{sq})_3$ (1). To a solution of the ligand $H_2[^{3,6}L_{cat}]$ (110 mg; 0.5 mmol) in acetonitrile (25 mL) was added $[CrCl_3(thf)_3]$ (62 mg; 0.17 mmol) followed by triethylamine (0.2 mL, 2 mmol). The reaction mixture was heated to reflux for 1 h in the presence of air, whereupon the color changed to red-purple. Slow evaporation of the solvent initiated the precipitation of crystalline **1**. Yield: 106 mg (90%). Anal. Calcd for $C_{42}H_{60}CrO_6$: C, 70.75; H, 8.48; Cr, 7.29. Found: C, 70.7; H, 8.5; Cr, 7.4.

$[Co(Cp)_2][Cr^{III}(^{3,6}L^{\bullet}_{sq})_2(^{3,6}L_{cat})]$ (2). To a deep violet solution of **1** (178 mg; 0.25 mmol) in CH_2Cl_2 (25 mL) under an argon atmosphere was added cobaltocene, $Co(Cp)_2$, (48 mg; 0.25 mmol).

(5) Pattison, D. I.; Levina, A.; Davies, M. J.; Lay, P. A. *Inorg. Chem.* **2001**, *40*, 214.
(6) Levina, A.; Foran, G. J.; Pattison, D. I.; Lay, P. A. *Angew. Chem., Int. Ed.* **2004**, *43*, 462.
(7) Milsmann, C.; Levina, A.; Harris, H. H.; Foran, G. J.; Turner, P.; Lay, P. A. *Inorg. Chem.* **2006**, *45*, 4743.
(8) Pierpont, C. G. *Inorg. Chem.* **2001**, *40*, 5727.
(9) Aliaga-Alcalde, N.; DeBeer, George, S.; Mienert, B.; Bill, E.; Wieghardt, K.; Neese, F. *Angew. Chem., Int. Ed.* **2005**, *44*, 2908.
(10) Belostotskaya, I. S.; Komissarova, N. L.; Dzhuaryan, E. V.; Ershov, V. V. *Isv. Akad. Nauk SSSR* **1984**, 1610.
(11) (a) Sellmann, D.; Freyberger, G.; Eberlein, R.; Böhlen, E.; Huttner, G.; Zsolnai, L. *J. Organomet. Chem.* **1987**, *323*, 21. (b) Sellmann, D.; Käppler, O. *Z. Naturforsch.* **1987**, *42b*, 1291.

After the reaction was stirred at 20 °C for 3 h, a blue precipitate of **2** formed which was isolated by filtration and washed with diethylether and air-dried. Yield: 185 mg (85%). Anal. Calcd for $C_{52}H_{70}CrO_6Co$: C, 69.24; H, 7.82; Cr, 5.76. Found: C, 69.1; H, 7.7; Cr, 5.7.

[N(*n*-bu)$_4$][Cr^{III}(^{3,5}L$^{\bullet}_{S,S}$)$_2$(^{3,5}L$_{S,S}$)] (3). To a solution of the ligand $H_2[^{3,5}L_{S,S}]$ (126 mg; 0.5 mmol) in acetonitrile (25 mL) was added $[CrCl_3(thf)_3]$ (46 mg; 0.125 mmol) under an Ar atmosphere. Triethylamine (0.3 mL; 3 mmol) was then added, and the solution was stirred at 20 °C for 1 h, after which time a stream of air was passed through the solution for 10 min. The color of the solution turned green. [N(*n*-bu)$_4$]Br (0.5 g) was then added. After the mixture stood at −20 °C, violet crystals of **3** were obtained which were filtered off and air-dried. Yield: 71 mg (55%). Anal. Calcd for $C_{58}H_{96}CrNS_6$: C, 66.96; H, 9.20; S, 18.29; Cr, 4.94. Found: C, 66.9; H, 9.1; S, 18.3; Cr, 4.9.

[As(Ph)$_4$][Cr^{V}O(^{3,5}L$_{S,S}$)$_2$] (4). The synthesis and crystallographic characterization of this species have been described previously.[12]

X-ray Absorption Spectroscopy. All data were measured at the Stanford Synchrotron Radiation Laboratory under ring conditions of 3.0 GeV and 60−100 mA. All S K-edge data were measured using the 54-pole wiggler beam line 6-2 in the high magnetic field mode of 10 kG with a Ni-coated harmonic rejection mirror and a fully tuned Si(111) double-crystal monochromator. Details of the optimization of this setup for low-energy studies have been described presiously.[13] Data were measured at room temperature by fluorescence, using a Lytle detector. To check for reproducibility, two to three scans were measured for each sample. The energy was calibrated from S K-edge spectra of $Na_2S_2O_3 \cdot 5H_2O$, run at intervals between sample scans. The maximum of the first pre-edge feature in the spectrum was fixed at 2472.02 eV. A step size of 0.08 eV was used over the edge region. Data were averaged, and a smooth background was removed from all spectra by fitting a polynomial to the pre-edge region and subtracting this polynomial from the entire spectrum. Normalization of the data was accomplished by fitting a flattened polynomial or straight line to the post-edge region (2490−2740 eV) and normalizing the post-edge to 1.0.

Cr K-edge XAS data were measured on unfocused bend magnet beam line 2-3 or focused 16-pole wiggler beam line 9-3. A Si(220) monochromator was utilized for energy selection. The monochromator was detuned 50% (for beam line 2-3) to minimize higher harmonic components in the X-ray beam (for beam line 9-3, a harmonic rejection mirror in combination with 25% detuning was used). All samples were prepared as solids in boron nitride, pressed into a pellet, and sealed between 38 μm Kapton tape windows in a 1 mm aluminum spacer. The samples were maintained at 10 K during data collection using an Oxford Instruments CF1208 continuous flow liquid helium cryostat. Data were measured in transmission mode. Internal energy calibrations were performed by simultaneous measurement of a Cr reference foil placed between a second and third ionization chamber. The first inflection point was assigned to 5989.0 eV. Data represent three to five scan averages and were processed by fitting a second-order polynomial to the pre-edge region and subtracting this background from the entire spectrum. A three-region cubic spline was used to model the smooth background above the edge. The data were normalized by subtracting the spline and normalizing the post-edge 1.0.

X-ray Crystallographic Data Collection and Refinement of the Structures. Dark brown single crystals of **1** and **3** were coated with perfluoropolyether, picked up with a glass fiber, and mounted in the nitrogen cold stream of a Bruker-Nonius Kappa-CCD diffractometer equipped with a Mo-target rotating-anode X-ray source and a graphite monochromator (Mo Kα, $\lambda = 0.71073$ Å). Final cell constants were obtained from least-squares fits of all measured reflections. The structures were readily solved by Patterson methods and subsequent difference Fourier techniques. The Siemens ShelXTL[14] software package was used for solution and artwork of the structure; ShelXL97[15] was used for the refinement. All non-hydrogen atoms were refined anisotropically. Hydrogen atoms were placed at calculated positions and refined as riding atoms with isotropic displacement parameters. Crystallographic data of the compounds are listed in Table 1.

Table 1. Crystallographic Data for **1** and **3**

	1	**3**
chem formula	$C_{42}H_{60}CrO_6$	$C_{58}H_{96}CrNS_6$
fw	712.90	1051.72
space group	*C*2/*c*, No. 15	$P2_1/c$, No. 14
a, Å	22.1182(9)	14.4072(8)
b, Å	19.1114(9)	21.579(2)
c, Å	10.0921(3)	20.1333(12)
β, deg	95.184(5)	90.703(5)
V, Å	4248.6(3)	6258.8(8)
Z	4	4
T, K	100(2)	100(2)
ρ_{calcd}, g cm^{-3}	1.115	1.116
reflns collected/2Θ_{max}	13 998/50.00	38 236/48.00
unique reflns/$I > 2\sigma(I)$	3727/2401	9790/6355
no. of params/restraints	222/0	617/0
λ, Å /μ(Kα), cm^{-1}	0.71073/3.10	0.71073/4.17
R1[a]/GOF[b]	0.0578/1.058	0.0685/1.059
wR2[c] ($I > 2\sigma(I)$)	0.1020	0.1358
residual density, e·Å^{-3}	+0.30/-0.34	+0.67/-0.42

[a] Observation criteria: $I > 2\sigma(I)$. $R1 = \sum||F_o| - |F_c||/\sum|F_o|$. [b] $GOF = [\sum[w(F_o^2 - F_c^2)^2]/(n-p)]^{1/2}$. [c] $wR2 = [\sum[w(F_o^2 - F_c^2)^2]/\sum[w(F_o^2)^2]]^{1/2}$ where $w = 1/\sigma^2(F_o^2) + (aP)^2 + bP$, $P = (F_o^2 + 2F_c^2)/3$.

Calculations. All calculations were performed by using the ORCA program package.[16] The geometry optimizations were carried out at either the B3LYP or BP86 level[17] of DFT. The all-electron Gaussian basis sets were those reported by the Ahlrichs group.[18,19] Triple-ζ quality basis sets with one set of polarization functions on the molybdenum, chromium, oxygen, and sulfur atoms were used (TZVP).[19] The carbon and hydrogen atoms were described by slightly smaller polarized split-valence SV(P) basis sets that is double-ζ quality in the valence region and contains a polarizing set of d functions on the non-hydrogen atoms.[18] The auxiliary basis sets for all complexes used to expand the electron density in the calculations were chosen to match the orbital basis. Scalar relativistic corrections for $[Mo^V(L_{S,S})_3]^-$ were included using the zeroth-order regular approximation (ZORA) method.[20] The SCF

(12) Kapre, R.; Ray, K.; Sylvestre, I.; Weyhermüller, T.; DeBeer, George, S.; Neese, F.; Wieghardt, K. *Inorg. Chem.* **2006**, *45*, 3499.
(13) Hedman, B.; Frank, P.; Gheller, S. F.; Roe, A. L.; Newton, W. E.; Hodgson, K. O. *J. Am. Chem. Soc.* **1988**, *110*, 3798.
(14) *ShelXTL V.5*; Siemens Analytical X-Ray Instruments, Inc.: Madison, WI, 1994.
(15) Sheldrick, G. M. *ShelXL97*; University of Göttingen: Göttingen, Germany, 1997.
(16) Neese, F. *ORCA, an Ab Initio, Density Functional and Semiempirical Electronic Structure Program Package, Version 2.4, Revision 36*; Max-Planck-Institut für Bioanorganische Chemie: Mülheim/Ruhr, Germany, May 2005.
(17) (a) Becke, A. D. *J. Chem. Phys.* **1988**, *84*, 4524. (b) Perdew, J. P. *Phys. Rev.* **1986**, *33*, 8522. (c) Lee, C.; Yang, W.; Parr, R. G. *Phys. Rev. B* **1988**, *37*, 785. (d) Becke, A. D. *J. Chem. Phys.* **1993**, *98*, 5648.
(18) Schäfer, A.; Horn, H.; Ahlrichs, R. *J. Chem. Phys.* **1992**, *97*, 2571.
(19) Schäfer, A.; Huber, C.; Ahlrichs, R. *J. Chem. Phys.* **1994**, *100*, 5829.
(20) (a) Van Wüllen, C. *J. Chem. Phys.* **1998**, *109*, 392. (b) van Lenthe, E.; Baerends, E. J.; Snijders, J. G. *J. Chem. Phys.* **1993**, *99*, 4597.

calculations were tightly converged (1×10^{-8} Eh in energy, 1×10^{-7} Eh in the density change and 1×10^{-7} in the maximum element of the DIIS error vector). The geometry search for all complexes was carried out in redundant internal coordinates without imposing geometry constraints. Corresponding orbitals[21] and density plots were obtained by the program Molekel.[22]

We describe our computational results of the molybdenum and chromium complexes containing noninnocent ligands using the BS approach first proposed by Ginsberg[23] and Noodleman.[24,25] The BS approach has been successfully applied for transition-metal-containing complexes in the past in the groups of Wieghardt, Neese,[26−30] and others.[24,31]

Since for some of the complexes studied in this work one can obtain BS solutions to the spin-unrestricted Kohn−Sham equations, we will adopt the following notation: the given system (molecule, ion) is divided into two fragments. The notation BS(m,n) then refers to a BS state with m unpaired spin-up electrons on fragment 1 and n unpaired spin-down electrons essentially localized on fragment 2. In most cases, fragments 1 and 2 correspond to the metal and the ligand, respectively. Note that in this notation a standard high-spin open-shell solution would be written down as BS($m + n$,0). In general, the BS(m,n) notation refers to the initial guess to the wavefunction. The variational process does, however, have the freedom to converge to a solution of the form BS($m - n$,0) where effectively the n spin-down electrons pair with $n < m$ spin-up electrons on the partner fragment. Such a solutionis then a standard $M_s \cong S = (m - n)/2$ unrestricted Kohn−Sham solution.

The calculations of $[Cr(L_{O,O})_3]^z$ ($z = 0, 1-, 2-, 3-$) were performed on the truncated models where the *tert*-butyl groups of the phenyl ring were substituted by hydrogen atoms. For $[Cr(^{3,5}L_{S,S})_3]^z$ ($z = 0, 1-, 2-, 3-$) and $[Mo(^{3,5}L_{S,S})_3]^{1-}$, nontruncated models were used.

Results and Discussion

Syntheses and Structural Characterization. From the reaction mixture of 3 equiv of the ligand 3,6-di-*tert*-butylcatechol, $H_2[^{3,6}L_{cat}]$, 1 equiv of $[Cr^{III}Cl_3(thf)_3]$, and 4 equiv of triethylamine in acetonitrile in the presence of air was obtained the purple, neutral complex **1** upon slow evaporation of the solvent.

Measurements of the magnetic susceptibility (3−300 K) showed that **1** is diamagnetic ($S = 0$). In the infrared spectrum, sharp and strong bands at 1432 and 1416 cm^{-1} are indicative of the presence of *o*-benzosemiquinonate(1−) π-radical anions.[1]

Reduction of **1** with 1 equiv of cobaltocene in CH_2Cl_2 solution under anaerobic conditions yielded blue microcrystals of **2**, which is paramagnetic (μ_{eff}(30−298 K) = 1.73 μ_B). The X-band EPR spectrum of **2** displays an isotropic signal at 10 K at $g = 1.976$ which is similar to other reported spectra of such spezies.[8] The $S = {}^1/_2$ ground state of **2** could be attained via intramolecular spin coupling between a central Cr(III) ion (d^3) and two *o*-semiquinonate(1−) radicals. Alternatively, Lay's[5−7] formulation as $[Cr^V(^{3,6}L_{cat})_3]^-$ must be considered. It is not possible to discern the two formulations by the above EPR spectrum.

Many reported attempts to synthesize tris(benzene-1,2-dithiolato)chromium species have resulted in the isolation of the monoanion $[Cr^V(bdt)_2(O)]^-$, which contains two closed shell benzene-1,2-dithiolato ligands, bdt^{2-}, a terminal oxo ligand, and a central chromium(V) ion (d^1).[32a] The only other reported tris(benzene-1,2-dithiolene)chromium complexes are $[NEt_4]_2[Cr(S_2C_6Cl_4)_3]$ ($S = 1$) and $[NEt_4][Cr(S_2C_6Cl_4)_3]$ ($S = {}^1/_2$), which have not been structurally characterized.[32b] The molecular and electronic structure of **4** ($S = {}^1/_2$) and $[N(n\text{-}Bu)_4][Cr^VO(tdt)_2]$ (tdt^{2-} = 4-methyl-1,2-benzenedithiolate) have been elucidated recently.[12]

We have now discovered that the reaction of 3 equiv of 3,5-di-*tert*-butyl-1,2-benzenedithiol, $H_2[^{3,5}L_{S,S}]$, with 1 equiv of $[Cr^{III}Cl_3(thf)_3]$ and 4 equiv of NEt_3 in acetonitrile under anaerobic conditions at 25 °C affords—after addition of excess $[N(n\text{-}Bu)_4]Br$ and subsequent exposure of the solutions to air for 10 min—violet crystals of **3** at −20 °C. The infrared spectrum of a solid sample (KBr disk) displays an intense $\nu(C{=}S^{\bullet})$ stretching frequency mode at 1108 cm^{-1} which has been identified previously as a marker for an S,S′-coordinated 3,5-di-*tert*-butyl-1,2-benzenedithiolate(1−) π radical.[33,34]

Magnetic susceptibility measurements (2−300 K) in a 1 T magnetic field revealed that **3** has a temperature-independent magnetic moment of 1.7 μ_B (50−300 K) as expected for an $S = {}^1/_2$ ground state. The X-band EPR spectrum of **3** in frozen CH_2Cl_2 at 10 K displays an axial signal with $g_\perp = 1.9947$ and $g_\parallel = 2.0074$.

The crystal structures of **1** and **3** have been determined by single-crystal X-ray crystallography at 100 K by using Mo Kα radiation. Figure 1 shows the structure of the neutral molecule in crystals of **1**, whereas Figure 2 displays the structure of the monoanion in crystals of **3**. The structure of

(21) Neese, F. *J. Phys. Chem. Solids* **2004**, *65*, 781.
(22) Molekel, Ed. *Molekel, Advance s Interactive 3d-Graphics for Molecular Sciences*; http://www.cscs.ch/molekel/.
(23) Ginsberg, A. P. *J. Am. Chem. Soc.* **1980**, *102*, 111.
(24) Noodleman, L.; Peng, C. Y.; Case, D. A.; Mouesca, J. M. *Coord. Chem. Rev.* **1995**, *144*, 199.
(25) (a) Noodleman, L.; Case, D. A.; Aizman, A. *J. Am. Chem. Soc.* **1988**, *110*, 1001. (b) Noodleman, L.; Davidson, E. R. *Chem. Phys.* **1986**, *109*, 131. (c) Noodleman, L.; Norman, J. G.; Osborne, J. H.; Aizman, C.; Case, D. A. *J. Am. Chem. Soc.* **1985**, *107*, 3418. (d) Noodleman, L. *J. Chem. Phys.* **1981**, *74*, 5737.
(26) (a) Bachler, V.; Olbrich, G.; Neese, F.; Wieghardt, K. *Inorg. Chem.* **2002**, *41*, 4179. (b) Ghosh, P.; Bill, E.; Weyhermüller, T.; Neese, F.; Wieghardt, K. *J. Am. Chem. Soc.* **2003**, *125*, 1293.
(27) (a) Herebian, D.; Bothe, E.; Neese, F.; Weyhermüller, T.; Wieghardt, K. *J. Am. Chem. Soc.* **2003**, *k125*, 9116. (b) Herebian, D.; Wieghardt, K.; Neese, F. *J. Am. Chem. Soc.* **2003**, *125*, 10997.
(28) Slep, L. D.; Mijovilovich, A.; Meyer-Klaucke, W.; Weyhermüller, T.; Bill, E.; Bothe, E.; Neese, F.; Wieghardt, K. *J. Am. Chem. Soc.* **2003**, *125*, 15554.
(29) Chlopek, K.; Bothe, E.; Neese, F.; Weyhermüller, T.; Wieghardt, K. *Inorg. Chem.* **2006**, *45*, 6298.
(30) Patra, A. K.; Bill, E.; Bothe, E.; Chlopek, K.; Neese, F.; Weyhermüller, T.; Stobie, K.; Ward, M. D.; McCleverty, J. A.; Wieghardt, K. *Inorg. Chem.* **2006**, *45*, 7877.
(31) (a) Remenyi, C.; Kaupp, M. *J. Am. Chem. Soc.* **2005**, *127*, 11399. (b) Bencini, A.; Carbonera, C.; Dei, A.; Vaz, M. G. F. *Dalton Trans.* **2003**, 1701.
(32) (a) Stiefel, E. I.; Eisenberg, R.; Rosenberg, R. C.; Gray, H. B. *J. Am. Chem. Soc.* **1966**, *88*, 2956. (b) Wharton, E. J.; McCleverty, J. A. *J. Chem. Soc. A* **1969**, 2258.
(33) (a) Petrenko, T.; Ray, K.; Wieghardt, K. E.; Neese, F. *J. Am. Chem. Soc.* **2006**, *128*, 4422.
(34) (a) Ray, K.; Weyhermüller, T.; Neese, F.; Wieghardt, K. *Inorg. Chem.* **2005**, *44*, 5345. (b) Ray, K.; Begum, A.; Weyhermüller, T.; Piligkos, S.; Neese, F.; Wieghardt, K. *J. Am. Chem. Soc.* **2005**, *127*, 4403. (c) Ray, K.; Bill, E.; Weyhermüller, T.; Wieghardt, K. *J. Am. Chem. Soc.* **2005**, *127*, 5641. (d) Ray, K.; Weyhermüller, T.; Goosens, A.; Crajé, M. W.; Wieghardt, K. *Inorg. Chem.* **2003**, *42*, 4082.

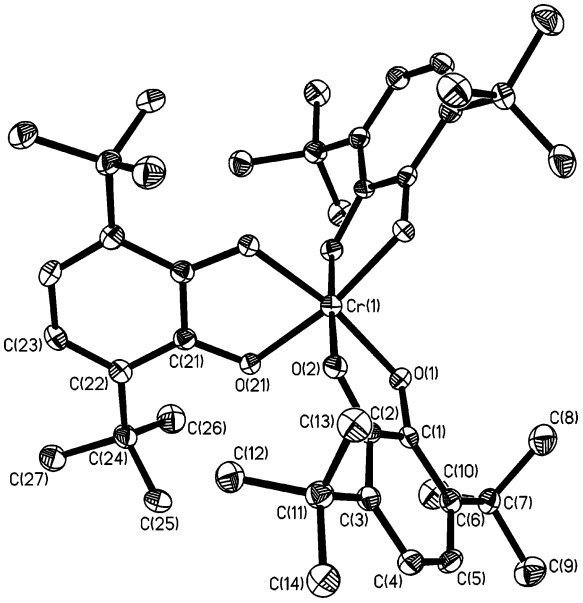

Figure 1. Structure of the neutral complex $[Cr^{III}(^{3,6}L^{\bullet}_{sq})_3]$ in crystals of **1**.

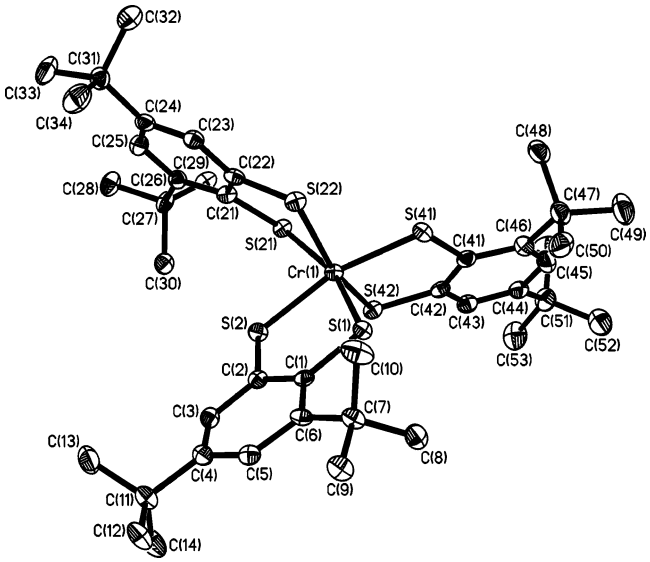

Figure 2. Structure of the monoanion $[Cr^{III}(^{3,5}L^{\bullet}_{S,S})_2(^{3,5}L_{S,S})]^-$ in crystals of **3**.

the oxochromium(V) species **4** has been reported.[12] Table 2 gives important bond distances and angles.

Crystals of **1** consist of neutral, slightly distorted octahedral molecules of $[Cr^{III}(^{3,6}L^{\bullet}_{sq})_3]$. The three O,O′-coordinated ligands are identical within experimental error, and the geometric details of these dioxolenes are typical for the *o*-semiquinonate(1−) oxidation level.[1−4] The average C−O bond distance at 1.306 ± 0.01 Å is intermediate between those of coordinated catecholates and quinones; they are the same as in previously reported neutral complexes of this kind.[35−37]

(35) Crystal structures of $[Cr^{III}(^{3,5}L^{\bullet}sq)_3]$, ref 2; $[Cr^{III}(O_2C_6Cl_4)_3]$, refs 3a, 36; and $[Cr^{III}(O_2C_6Br_4)_3]$, ref 37.
(36) (a) Buchanan, R. M.; Kessel, S. L.; Downs, H. H.; Pierpont, C. G.; Hendrickson, D. N. *J. Am. Chem. Soc.* **1978**, *100*, 7894.
(37) Chang, H.-C.; Ishii, T.; Kondo, M.; Kitagawa, S. *J. Chem. Soc., Dalton Trans.* **1999**, 2467.

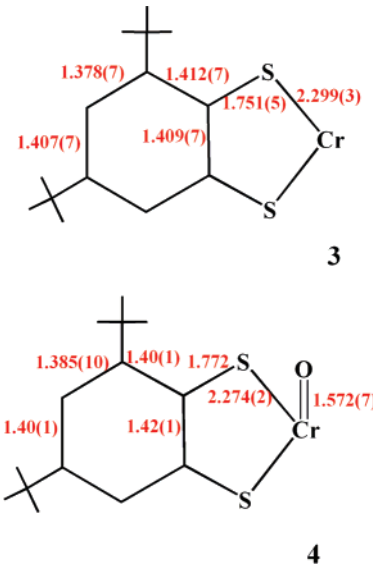

Figure 3. Comparison of average bond lengths (Å) in **3** and **4**.

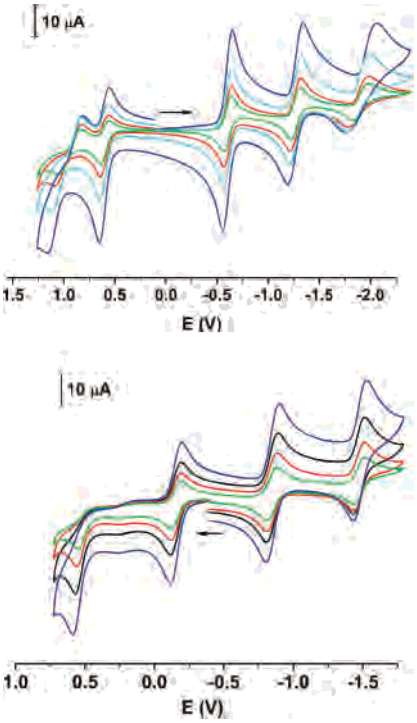

Figure 4. Cyclic voltammograms of **1** (top) and **3** (bottom) in CH_2Cl_2 solution (0.10 M $[N(n\text{-}Bu)_4]PF_6$) at 22 °C at scan rates 50, 100, 200, and 400 mV s^{-1} (glassy carbon working electrode). Potentials are referenced vs the Fc^+/Fc couple.

Furthermore, the phenyl rings display the typical quinoid-type distortion of coordinated *o*-semiquinones, namely two alternating short C−C bonds at 1.372 ± 0.01 Å and four longer C−C bonds at 1.430 ± 0.01 Å.

The average Cr−O distance in **1** at 1.937 ± 0.006 Å is very similar to that observed in $[Fe(Cp)_2][Cr^{III}(Cl_4\text{-}Sq)_2(Cl_4\text{-}Cat)]\cdot C_6H_6$ at 1.941 ± 0.01 Å or in $[Co(Cp)_2]_2[Cr^{III}(Br_4\text{-}SQ)(Br_4\text{-}Cat)_2]$ at 1.943 ± 0.01 Å.[4] The latter data agree extraordinarily well with Lay's EXAFS data[7] for the monoanion at 1.937(5) Å and the dianion at 1.943(5) Å. Thus, the average Cr−O distance in the neutral compound, monoanion, and dianion are the same regardless of the

Table 2. Selected Bond Distances (Å) and Angles (deg) of **1** and **3**

		Complex **1**			
Cr(1)−O(1)	1.929(2)	O(2)−C(2)	1.305(4)	C(2)−C(3)(	1.433(4)
Cr(1)−O(2)	1.934(2)	O(21)−C(21)	1.303(4)	C(3)−C(4)	1.372(4)
Cr(1)−O(21)	1.947(2)	C(1)−C(2)	1.440(4)	C(4)−C(5)	1.420(5)
O(1)−C(1)	1.310(4)	C(1)−C(6)	1.431(4)	C(5)−C(6)	1.372(4)
O(1)−Cr(1)−O(2)	81.41(9)	O(1)#−Cr(1)−O(2)#1	81.41(9)	O(1)−Cr(1)−O(21)#1	169.25(9)
O(21)#1−Cr(1)−O(21)	81.4(9)	O(1)#1−Cr(1)−O(21)	169.25(9)	O(2)−Cr(1)−O(2)#1	177.7(1)
		Complex **3**			
Cr(1)−S(1)	2.283(1)	Cr(1)−S(21)	2.301(1)	Cr(1)−S(41)	2.304(1)
Cr(1)−S(2)	2.290(1)	Cr(1)−S(22)	2.327(1)	Cr(1)−S(42)	2.291(1)
S(1)−C(1)	1.754(5)	S(2)−C(21)	1.756(5)	S(41)−C(41)	1.757(5)
S(2)−C(2)	1.746(5)	S(22)−C(22)	1.753(5)	S(42)−C(42)	1.738(5)
C(1)−C(2)	1.408(7)	C(21)−C(22)	1.412(7)	C(41)−C(42)	1.406(7)
C(1)−C(6)	1.411(7)	C(21)−C(26)	1.422(7)	C(41)−C(46)	1.432(7)
C(2)−C(3)	1.401(7)	C(22)−C(23)	1.399(7)	C(42)−C(43)	1.409(7)
C(3)−C(4)	1.363(7)	C(23)−C(24)	1.374(7)	C(43)−C(44)	1.364(7)
C(4)−C(5)	1.410(7)	C(24)−C(25)	1.404(7)	C(44)−C(45)	1.408(7)
C(5)−C(6)	1.397(7)	C(25)−C(26)	1.385(7)	C(45)−C(46)	1.386(8)
S(1)−Cr(1)−S(2)	84.49(5)	S(21)−Cr(1)−S(22)	83.85(5)	S(42)−Cr(1)−S(41)	84.37(3)
S(1)−Cr(1)−S(21)	163.11(6)	S(2)−Cr(1)−S(41)	164.97(6)	S(42)−Cr(1)−S(22)	159.58(6)

Table 3. Redox Potentials of Complexes at 22 °C in V vs Fc^+/Fc in CH_2Cl_2 Solution (0.10 M $[N(n\text{-}Bu)_4]PF_6$)

complex	$E^1_{1/2}$ (3−/2−)	$E^2_{1/2}$ (2−/1−)	$E^3_{1/2}$ (1−/0)	$E^4_{1/2}$ (0/1+)	$E^5_{1/2}$ (1+/2+)
1	−1.93	−1.29	−0.63	+0.58	+0.97
3	−1.57	−0.94	−0.25	+0.46	−
4[a]	−	−0.96	+0.15(q.r.)	−	−
$[N(n\text{-}Bu)_4][Mo^V(^{3,5}L_{S,S})_3]$[b]	−	−0.99	−0.48	+0.91 (irr.)	−

[a] Reference 12. [b] Reference 38.

method of determination (X-ray or EXAFS). It is only in the trianion $[Cr^{III}(L_{cat})_3]^{3-}$ that a longer average Cr−O distance at 1.980(5) Å has been observed by X-ray crystallography and EXAFS.[2b,7]

Crystals of **3** consist of well-separated tetra-*n*-butylammonium cations and $[Cr(^{3,5}L_{S,S})_3]^-$ anions. The structure of complex **3** represents the first crystallographically characterized tris(benzene-1,2-dithiolato)chromium species. The CrS_6 polyhedron adopts a geometry intermediate between a regular octahedron ($\theta = 60°$) and a trigonal prism ($\theta = 0$) where the twist angle θ is the chelate projection angle. In the present CrS_6 polyhedron, the three twist angles θ are at 46.0°, 37.7°, and 33.7° ($\theta_{av} = 39.1°$). Interestingly, in isostructural $[N(n\text{-}Bu)_4][Mo^V(^{3,5}L_{S,S})_3]\cdot CH_3CN$,[38] the MoS_6 polyhedron is also intermediate between regular octahedral and trigonal prismatic with an average $\theta = 31.7°$. Here it has been shown by S K-edge XAS that the three ligands are all closed-shell dianions $(^{3,5}L_{S,S})^{2-}$ rendering the central metal ion a Mo(V) (d^1).[38]

The bending angles α, α′, and α″ between the CrS_2 planes and the S_2C_2 planes of the ligands $(^{3,5}L_{S,S})^{n-}$ are irregular at 12.9°, 23.6°, and 6.5° in **3**. These are again very similar in $[Mo^V(^{3,5}L_{S,S})_3]^-$ (13.6°, 23.9°, 3.3°).

It is now interesting to compare the geometries of the five-membered chelate rings in **3** and the genuine Cr(V) complex **4**.[12] As shown in Figure 3, the average Cr−S distances in both structures are similar: 2.299(3) Å in **3** and 2.274(2) Å in **4**.

(38) Kapre, R. R.; Bothe, E.; Weyhermüller, T.; DeBeer George, S.; Wieghardt, K. *Inorg. Chem.* **2007**, *46*, 5642.

They are slightly shorter in **4** due to the higher oxidation state of the central Cr(V) ion and the lower coordination number as compared to **3**. Thus, it is not possible to assign spectroscopic oxidation states of the chromium ion or determine the oxidation level of the benzene-1,2-dithiolate ligands by X-ray crystallography (or EXAFS) within experimental error (3σ). Having said this, it is noticeable that the average geometries of the $(^{3,5}L_{S,S})^{2-}$ ligands in **3** and **4** differ slightly: in **4** the average C−S distance at 1.77 ± 0.01 Å is long and typical for $(^{3,5}L_{S,S})^{2-}$ ligands; in contrast, in **3** the shorter average C−S distance at 1.75 ± 0.01 Å points to the presence of one or two π-radical monoanions $(^{3,5}L^{\bullet}_{S,S})^{1-}$. The quinoid-type distortion of the phenyl rings in **3** also points to this interpretation.

Electro- and Spectroelectrochemistry. Figure 4 shows the cyclic voltammograms of **1** (top) and **3** (bottom) in CH_2Cl_2 solution containing 0.10 M $[N(n\text{-}Bu)_4](PF_6)$ supporting electrolyte at 22 °C at a glassy carbon working electrode. All redox potentials are referenced versus the ferrocenium/ferrocene couple (Fc^+/Fc). Table 3 summarizes the results.

The cyclic voltammogram of **1** displays three successive, fully reversible one-electron reduction waves ($E^{1-3}{}_{1/2}$) and two reversible, one-electron oxidations ($E^{4-5}{}_{1/2}$). Thus, the neutral species **1** may form a mono-, di-, and trianion $[\mathbf{1}]^{1-}$, $[\mathbf{2}]^{2-}$, $[\mathbf{1}]^{3-}$ and a mono-, and dication $[\mathbf{1}]^{1+}$ and $[\mathbf{1}]^{2+}$. The charge distribution in these species has traditionally been described as shown in eq 4 and, more recently, by Lay et al. as in eq 5,[5−7] where BQ represents a neutral benzoquinone, $(SQ)^{1-}$ a monoanionic *o*-benzosemiquinonate(1−), and $(Cat)^{2-}$ the catecholate(2−) dianion.

$$[Cr^{III}(BQ)_2(SQ^{\bullet})]^{2+} \underset{-e}{\overset{+e}{\rightleftharpoons}} [Cr^{III}(BQ)(SQ^{\bullet})_2]^{1+} \underset{-e}{\overset{+e}{\rightleftharpoons}} [Cr^{III}(SQ^{\bullet})_3]^{0} \underset{-e}{\overset{+e}{\rightleftharpoons}} [Cr^{III}(Cat)(SQ^{\bullet})_2]^{1-} \underset{-e}{\overset{+e}{\rightleftharpoons}} [Cr^{III}(Cat)_2(SQ^{\bullet})]^{2-} \underset{-e}{\overset{+e}{\rightleftharpoons}} [Cr^{III}(Cat)_3]^{3-} \quad (4)$$

$$S = 1 \qquad S = 1/2 \qquad S = 0 \qquad S = 1/2 \qquad S = 1 \qquad S = 3/2$$

$$[Cr^{III}(SQ^{\bullet})_3]^{0} \underset{-e}{\overset{+e}{\rightleftharpoons}} [Cr^{V}(Cat)_3]^{-} \underset{-e}{\overset{+e}{\rightleftharpoons}} [Cr^{IV}(Cat)_3]^{2-} \underset{-e}{\overset{+e}{\rightleftharpoons}} [Cr^{III}(Cat)_3]^{3-} \quad (5)$$

$$S = 0 \qquad S = 1/2 \qquad S = 1 \qquad S = 3/2$$

Note that the couple $z = 0/1-$ involves either two Cr(III) species in the traditional interpretation eq 4 containing three *o*-semiquinonate(1−) π radicals and/or only two π radicals and one catecholate ligand or, alternatively, a Cr(III) and Cr(V) species and three catecholate ligands in both species according to Lay et al.[7] as shown in eq 5. Similar voltammograms have been reported for all other such tris(dioxolene)chromium complexes.[1−7]

In the potential range +0.25 to −2.0 V the cyclic voltammogram of the tris(dithiolene)chromium complex **3** exhibits three reversible, successive one-electron transfer waves, as shown in eq 6. The monoanion can be oxidized

$$[Cr^{III}(^{3,5}L^{\bullet}_{S,S})_3]^{0} \underset{-e}{\overset{+e}{\rightleftharpoons}} [Cr^{III}(^{3,5}L^{\bullet}_{S,S})_2(^{3,5}L_{S,S})]^{1-} \underset{-e}{\overset{+e}{\rightleftharpoons}} [Cr^{III}(^{3,5}L^{\bullet}_{S,S})(^{3,5}L_{S,S})_2]^{2-}$$

$$S = 0 \qquad E^3_{1/2} \qquad S = {}^1/_2 \qquad E^2_{1/2} \qquad -e\uparrow\downarrow+e \qquad E^1_{1/2} \qquad (6)$$

$$[Cr^{III}(^{3,5}L_{S,S})_3]^{3-}$$

to the neutral species and twice reduced to the di- and trianion, respectively.

An irreversible oxidation wave is observed at +0.46 V which we have not investigated in further detail.

Figure 5 exhibits the electronic spectra of the neutral complex **1** and of its electrochemically generated mono-, di-, and trianion in CH_2Cl_2 solution at −5 °C, whereas Figure 6 displays the corresponding series of spectra of the sulfur-containing compounds $[\mathbf{3}]^0$, $[\mathbf{3}]^{1-}$, $[\mathbf{3}]^{2-}$, and $[\mathbf{3}]^{3-}$. Table 4 summarizes the spectra.

The electronic spectra of **1**, $[\mathbf{1}]^{1-}$, $[\mathbf{1}]^{2-}$, and $[\mathbf{1}]^{3-}$ resemble closely those reported previously[1−4] for other tris(dioxolene)-chromium complexes. It is remarkable that the spectra of the monoanion and of the dianion exhibit very intense absorption maxima in the near-infrared at 1700 nm for $[\mathbf{1}]^{1-}$ and at 1480 nm for $[\mathbf{1}]^{2-}$. These bands have been assigned by Kitagawa et al.[4a] as ligand-based intervalence charge transfer (IVCT) bands which are observed only if both oxidation levels of the ligands, namely an *o*-semiquinone and a catecholate, are present. In neutral **1** containing three *o*-semiquinonates(1−) and in $[\mathbf{1}]^{3-}$ containing three catecholates(2−) ligands, this NIR transition is absent. It is not possible to assign these intense mixed-ligand IVCT bands to d−d transitions of putative $[Cr^{V}(cat)_3]^{-}$ and $[Cr^{IV}(cat)_3]^{2-}$ complexes.

It is very revealing that the electronic spectra of $[\mathbf{3}]^0$, $[\mathbf{3}]^{1-}$, $[\mathbf{3}]^{2-}$, and $[\mathbf{3}]^{3-}$ are remarkably similar to those of their

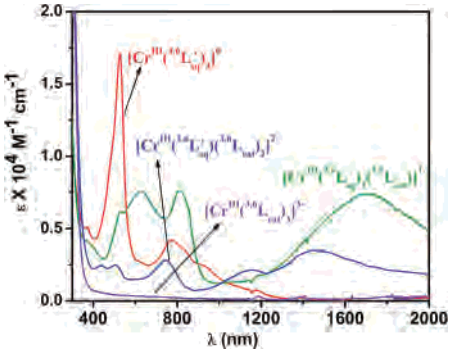

Figure 5. Electronic spectra of neutral **1** and electrochemically generated $[\mathbf{1}]^{1-}$,$[\mathbf{1}]^{2-}$, and $[\mathbf{1}]^{3-}$ in CH_2Cl_2 solution (0.10 M $[N(n\text{-}Bu)_4]PF_6$) at −5 °C.

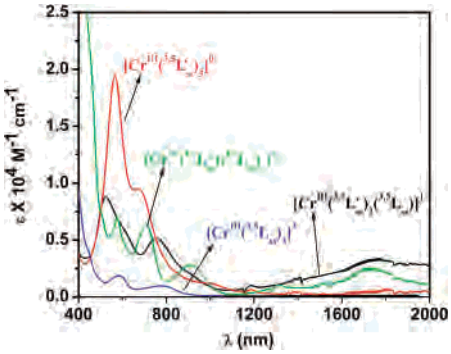

Figure 6. Electronic spectra of **3** and electrochemically generated $[\mathbf{3}]^0$, $[\mathbf{3}]^{2-}$, and $[\mathbf{3}]^{3-}$ in CH_2Cl_2 solution (0.10 M $[N(n\text{-}Bu)_4]PF_6$) at −5 °C.

Table 4. Electronic Spectra of Complexes in CH_2Cl_2 Solution (0.10 M $[N(n\text{-}Bu)_4]PF_6$) at −5 °C in the Range 300−2000 nm

complex	λ_{max}, nm ($10^4\ \epsilon$, $M^{-1}\ cm^{-1}$)
[**1**]	392(0.5), 500sh, 530(1.74), 630sh, 790(0.7), 810sh, 920sh
$[\mathbf{1}]^{1-}$	400(0.4), 530(0.6), 620(0.75), 810(0.75), 1700(0.8)
$[\mathbf{1}]^{2-}$	420(0.25), 505(0.25), 750(0.3), 1150sh, 1480(0.35)
$[\mathbf{1}]^{3-}$	no absorption maxima with $\epsilon > 0.2 \times 10^3\ M^{-1}\ cm^{-1}$
$[\mathbf{3}]^{0}$	590(2.0), 700(0.9), 1000(0.2)
$[\mathbf{3}]^{1-}$	520(0.8), 600sh, 780(0.5), 910sh, 1750(0.3)
$[\mathbf{3}]^{2-}$	500sh, 590(0.7), 610sh, 700(0.6), 910(0.3), 1720(0.25)
$[\mathbf{3}]^{3-}$	460(0.4)sh, 590(0.2), 790(0.15)
$[Mo^{V}(^{3,5}L_{S,S})_3]^{-}$ [a]	413(1.6), 479(1.2), 638(0.9), 701(0.8)

[a] Reference 12.

oxygen analogues above. The spectrum of the trianion $[\mathbf{3}]^{3-}$ exhibits two d−d transitions of relatively low intensity in the visible at 590 and 790 nm, as is typical for octahedral chromium(III) species. The electronic structure of this species is best described as $[Cr^{III}(^{3,5}L_{S,S})_3]^{3-}$ with a chromium(III) central ion (d^3, $S = {}^3/_2$) and three closed-shell dithiolate-(2−) ligands.

Since the spectra of the neutral species **1** and the electrochemically generated neutral $[\mathbf{3}]^0$ are also very similar, we propose the same electronic structure for both species, namely $[Cr^{III}(^{3,6}L^{\bullet}_{sq})_3]^0$ and $[Cr^{III}(^{3,5}L^{\bullet}_{S,S})_3]^0$. Thus, both complexes have a central Cr(III) ion and three π-radical monoanionic ligands which couple antiferromagnetically yielding the observed $S = 0$ ground state in both compounds.

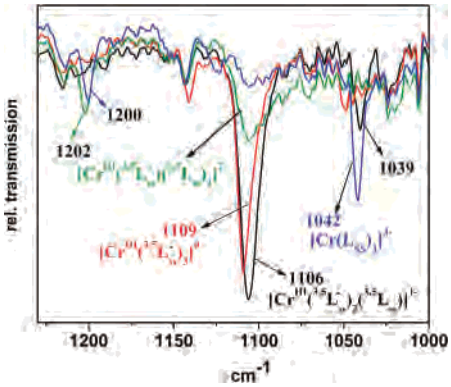

Figure 7. Changes in the infrared spectra upon oxidation and reduction of **3** in CH_2Cl_2 solution in the range 1000−1250 cm^{-1}.

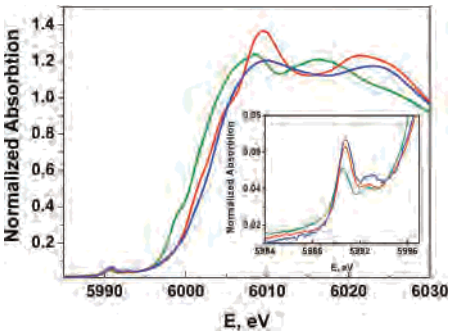

Figure 8. Comparison of the normalized Cr K-edge data for **1** (red), **2** (blue), and *trans*-$[CrCl_2(OH_2)_4]Cl$ (green). The inset shows an expansion of the pre-edge region.

It is now gratifying that the spectra of the mono- and dianions, $[\mathbf{3}]^{1-}$ and $[\mathbf{3}]^{2-}$, display a relatively intense IVCT band at 1750 and 1720 nm, respectively. Thus, their electronic structure is very similar to those of $[\mathbf{1}]^{1-}$ and $[\mathbf{2}]^{2-}$ and involves ligand-mixed valency.

It has been possible to record the infrared spectra of $[\mathbf{3}]^{1-}$ and its electrochemically generated neutral complex, as well as the di- and trianion, in CH_2Cl_2 solution in the range 1250−1000 cm^{-1}; they are shown in Figure 7. The solid-state infrared spectrum (KBr) of **3** displays an intense $\nu(C{=}S^{\bullet})$ stretching frequency at 1117 cm^{-1}, which is shifted to 1106 cm^{-1} in CH_2Cl_2 solution. This band has been previously identified as a marker for the presence of the π-radical anion $(^{3,5}L^{\bullet}_{S,S})^{1-}$ in coordination compounds.[33,34] Interestingly, upon one-electron oxidation generating the neutral species $[\mathbf{3}]^0$, this band shifts to 1109 cm^{-1}, whereas upon one-electron reduction generating the dianion $[\mathbf{3}]^{2-}$, this band at 1106 cm^{-1} looses intensity, and in the trianion $[\mathbf{3}]^{3-}$ this mode is absent. Conversely, a $\nu(C-S)$ mode of a coordinated closed-shell dithiolate(2−) at 1042 cm^{-1} in $[\mathbf{3}]^{3-}$ loses intensity in $[\mathbf{3}]^{1-}$ (it has not been observed in the spectrum of $[\mathbf{3}]^{2-}$). These observations clearly indicate that the redox processes are ligand- rather than metal-centered.

X-ray Absorption Spectroscopy. Cr K-Edge XAS. Figure 8 displays a comparison of the normalized Cr K-edge data of solid samples of *trans*-$[Cr^{III}Cl_2(OH_2)_4]Cl$, **1**, and **2**. Because of the presence of two-electron ligand-to-metal charge-transfer transitions in the ∼5995−6005 eV range, the rising edge regions are difficult to compare. However, the pre-edge can be used as an indication of the oxidation state trends. The pre-edge energy of *trans*-$[CrCl_2(OH_2)_4]Cl$ is found at 5990.6 and 5992.7 eV with an area of 6.2; that of **1** is at 5990.7, 5992.8 eV (area = 7.3), and that of **2** is at 5990.7, 5992.9 eV (area = 9.2). *This set of data clearly indicates that the oxidation state of the central chromium ion in trans-[CrCl2(OH2)4]Cl, 1, and 2 remains the same, namely +III.* We do not observe an ∼2 eV shift to higher energy on going from **1** to **2**, as might be expected upon reduction of neutral $[Cr^{III}(SQ)_3]^0$ to a $[Cr^{V}(cat)_3]^-$ ion according to Lay et al.[5−7]

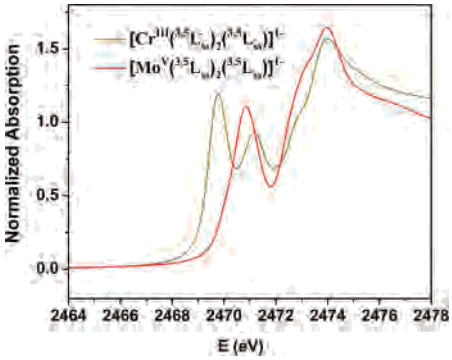

Figure 9. Comparison of S K-edges for **3** (brown) and $[Mo^{V}(^{3,5}L_{S,S})_3]^-$ (red).

The Cr pre-edge peak for **3** (5989.7, 5990.8 eV) appears at ∼0.9 eV lower energy than that of the reference Cr(III) complex, **1**, and **2**. The area of 13.6 is larger, indicating the presence of significantly covalent Cr−S bonds in **3**. This effect is due to a decreased effective nuclear charge at the chromium ion which is caused by the presence of six soft (π-donating) sulfur donors in **3** vs six harder oxygen donors in **1** and **2**. As we will show below, a description as $[Cr^{II}(^{3,5}L^{\bullet}_{S,S})_3]^-$ is not appropriate and a description as $[Cr^{V}(^{3,5}L_{S,S})_3]^-$ is out of the question. We note that the electronic spectra of complexes $[Cr^{III}(^{3,6}L^{\bullet}_{sq})_2(^{3,6}L_{cat})]^-$ and its sulfur-containing analogue $[Cr^{III}(^{3,5}L^{\bullet}_{S,S})_2(^{3,5}L_{S,S})]^-$ in Figures 5 and 6, respectively, are very similar. They are quite different from that reported for $[Mo^{V}(^{3,5}L_{S,S})_3]^-$ in ref 38 which contains a genuine Mo(V) (d^1) ion and three closed-shell $(^{3,5}L_{S,S})^{2-}$ ligands.

S K-Edge XAS. Figure 9 shows a comparison of the S K-edge spectrum of the monoanion in crystals of **3** and that of isostructural $[N(n\text{-}Bu)_4][Mo^{V}(^{3,5}L_{S,S})_3]$. The latter spectrum displays an intense single pre-edge feature at ∼2470.8 eV which is typical for S,S-coordinated, closed-shell benzene-1,2-dithiolates(2−).[39,40] In stark contrast, the spectrum of **3** exhibits *two* pre-edge peaks, a lower energy feature at ∼2469.8 eV and a higher energy feature at 2471.2 eV. The new, intense, lower pre-edge feature at ∼2469.8 eV is assigned a S 1s-to-3p transition reflecting ligand π-radical

(39) (a) Szilagyi, R. K.; Lim, B. S.; Glaser, T.; Holm, R. H.; Hedman, B.; Hodgson, K. O.; Solomon, E. I. *J. Am. Chem. Soc.* **2003**, *125*, 9158. (b) Sarangi, R.; DeBeer, George, S.; Rudd, D. J.; Szilagyi, R. K.; Ribas, X.; Rovira, C.; Almeida, M.; Hodgson, K. O.; Hedman, B.; Solomon, E. I. *J. Am. Chem. Soc.* **2007**, *129*, 2316.
(40) Ray, K.; DeBeer, George, S.; Solomon, E. I.; Wieghardt, K.; Neese, F. *Chem. Eur. J.* **2007**, *13*, 2754.

character.[39,40] Interestingly, the S K-edge of chromium complex **3** exhibits an increased rising edge energy relative to the molobdenum(V) species. This is also consistent with a ligand-based oxidation in **3**. Therefore, the electronic structure of the monoanion in **3** is best described as $[Cr^{III}(^{3,5}L^{\bullet}_{S,S})_2(^{3,5}L_{S,S})]^-$.

Calculations. In this section, a picture of the electronic structures of the complexes $[Cr(L_{O,O})_3]^z$ and $[Cr(^{3,5}L_{S,S})]^z$ ($z = 0, 1-, 2-, 3-$) is derived from BS DFT calculations by using the B3LYP functional for geometry optimizations, the MO descriptions, and spin distributions in these complexes. In order to be able to compare our calculations with those reported for $[Cr(L_{O,O})_3]^{1-,2-,3-}$ by Lay et al.[7] we have also performed calculations using the BP86 functional, where $(L_{O,O})$ represents an unsubstituted benzene-1,2-dioxolene ligand. The main difference between our and Lay et al.'s calculations is the use of the BS approach[23−25] in our calculations. By using the BP86 functional and spin-unrestricted solutions as reported by Lay et al.,[7] we have been able to fully reproduce their reported data with Neese's ORCA program package.[16] In general, we found that the optimized geometries of all calculated complexes using either the BP86 (spin-unrestricted) or the B3LYP functional (BS) agree very well but the Mulliken spin population analyses differ significantly in both approaches.

Calculated Geometries. Consistent with the notion that the distorted octahedral complexes of the series $[Cr(L_{O,O})_3]^z$ and of the corresponding sulfur complexes $[Cr(^{3,5}L_{S,S})_3]^z$ ($z = 0, 1-, 2-$) contain three, two, and one radical ligands, the ground state geometries for these molecules were optimized in the high-spin states ($S = 3, {}^5/_2, 2$) and in the corresponding BS states $M_s = 0, {}^1/_2$, and 1 by using the B3LYP functional. The geometry of the trianions $[Cr^{III}(L_{cat})_3]^{3-}$ and $[Cr^{III}(^{3,5}L_{S,S})_3]^{3-}$ and of the monoanion $[Mo^{V}(^{3,5}L_{S,S})_3]^-$ were calculated spin-unrestricted ($S_t = {}^3/_2, {}^3/_2$, and ${}^1/_2$, respectively). Although describing different electronic structures, the bond lengths in the high- and low-spin geometries for the neutral, monoanionic, and dianionic complexes of both series are very similar and are very close to those of the experimental structures (Supporting Information).

The calculated geometry and metrical parameters of the species $[Cr(L_{O,O})_3]^z$ ($z = 0, 1-, 2-, 3-$) and of $[Cr(^{3,5}L_{S,S})_3]^-$ are found to be in good agreement with experimental values (Supporting Information). The intermediate octahedral-trigonal prismatic geometry of all dioxolene complexes (average twist angle $\theta \approx 50°$) is well reproduced. For the sulfur-containing monoanion $[Cr(^{3,5}L_{S,S})_3]^-$, the experimental twist angle at 39.1° is not quite as accurately reproduced in the calculation ($\theta_{calcd} \approx 47.5°$).

It is now interesting that the experimental average Cr−O bond distances in the neutral complex, monoanion, and dianion are within experimental error of 3σ identical at ∼1.94 ± 0.01 Å whereas in the trianion this distance is longer at 1.98 ± 0.01 Å. This trend has been well reproduced by the present calculations where an average value of 1.98 Å for the first three species and one at 2.03 Å for the trianion has been calculated. The overestimation of the calculated Cr−O bond distance of consistently 0.05 Å is typical for the B3LYP functional. Similarly, the experimental average Cr−S distance in the monoanion of **3** at 2.299 ± 0.003 Å is shorter by 0.086 Å than the calculated one.

Table 5. Average Bond Distances in $[N(n\text{-}Bu)_4][Mo^{V}(^{3,5}L_{S,S})_3]$ and **3**

	$[Mo^{V}(^{3,5}L_{S,S})_3]^-$		$[Cr^{III}(^{3,5}L^{\bullet})_2(^{3,5}L_{S,S})]^-$	
	exptl, Å	calcd, Å	exptl, Å	calcd, Å
M−S	2.376	2.416	2.299	2.385
C−S	1.757(3)	1.771	1.751	1.755
C(1)−C(2)	1.407(4)	1.416	1.409	1.431
C(1)−C(6)	1.421(4)	1.430	1.422	1.440
C(2)−C(3)	1.396(4)	1.404	1.403	1.411
C(3)−C(4)	1.382(4)	1.394	1.367	1.388
C(4)−C(5)	1.407(4)	1.408	1.407	1.413
C(5)−C(6)	1.396(4)	1.404	1.389	1.399
θ, deg[a]	29.7	34.2	46.0	47.1
θ', deg[a]	39.9	35.2	37.7	46.9
θ'', deg[a]	25.4	35.2	33.7	48.6
α, deg[b]	13.6	4.3	12.6	3.6
α', deg[b]	23.9	3.9	23.6	2.6
α'', deg[b]	3.3	4.3	6.5	4.7

[a] Twist angle. [b] Dihedral bending angle between C_2S_2 and MS_2 planes of S,S-coordinated ligand.

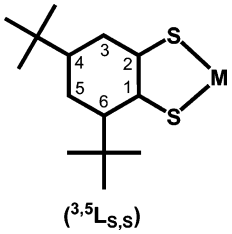

$(^{3,5}L_{S,S})$

It is gratifying that the observed geometry of the three catecholate(2−) ligands in the trianion $[Cr(L_{O,O})_3]^{3-}$ is closely reproduced by the calculations: The average C−C distance in the aromatic ring is at 1.413 Å, and no chinoid-type distortion is detected. The C−O bonds at 1.31 Å are indicative of the catecholate(2−) oxidation level and are in reasonable agreement with experiment (1.34 Å).

In contrast, in the neutral complex $[Cr(L_{O,O})_3]^0$, the three ligands are clearly benzo-1,2-semiquinonates(1−). The three rings exhibits quinoid-type distortions and the C−O bonds are short at 1.29 Å (in **1**, 1.305 Å).

These results clearly point to a central chromium(III) (d^3) ion in both **1** and $K_3[Cr^{III}(cat)_3]$.[2] The calculated structures of the monoanion and dianion show that both ions contain three equivalent ligands, the oxidation level of which cannot unambiguously be derived from the experimental or the calculated geometries of the ligands. It is remarkable that the calculations faithfully reproduce the experimental data for both species.

The calculated structure of the monoanion $[Mo^{V}(^{3,5}L_{S,S})_3]^-$ also agrees well that determined experimentally[38] (Table 5). Clearly, three equivalent 3,5-di-*tert*-butylbenzene-1,2-dithiolato(2−) ligands are present with long average C−S bonds at 1.77 Å and nondistorted aromatic phenyl rings. An average calculated twist angle θ of 35° is slightly overestimated as compared to experiment (31.7°). The average bending angles α between the MoS_2 and S_2C_2 planes at 13.6° (exptl) and 4.2° (calcd) agree reasonably well.

Electronic Structures. The Trianions. The spin-unrestricted BP86 and B3LYP calculated electronic structure of

Table 6. Selected DFT Calculated Spin Densities (B3LYP)

	S_t	Mulliken metal atom spin density	Mulliken ligand spin density for all three ligands	J, cm^{-1} [g]
$[Cr^{III}(L_{cat})_3]^{3-}$	$^3/_2$	3.03[b] (2.98)[a]	~0 (~0)[a]	
$[Cr^{III}(L^{\bullet}_{sq})(L_{cat})_2]^{2-}$	1	2.80[e] (2.34)[a]	−0.47 (−0.34)[a]	−527
$[Cr^{III}(L^{\bullet}_{sq})_2(L_{cat})]^{-}$	$^1/_2$	2.83[d] (1.89)[a]	−1.80 (−0.89)[a]	−606
$[Cr^{III}(L^{\bullet}_{sq})_3]^{0}$	0	2.93[c] (2.19)[f]	−3.06 (−2.19)[f]	−475
$[Cr^{III}(^{3,5}L^{\bullet}_{S,S})_3]^{0}$	$^3/_2$	3.03[c]	−2.79	−732
$[Cr^{III}(^{3,5}L^{\bullet}_{S,S})_2(^{3,5}L_{S,S})]^{-}$	$^1/_2$	3.04[d]	−1.80	−714
$[Cr^{III}(^{3,5}L^{\bullet}_{S,S})(^{3,5}L_{S,S})_2]^{2-}$	1	3.04[e]	−1.00	−175
$[Cr^{III}(^{3,5}L_{S,S})_3]^{3-}$	$^3/_2$	3.22[b]	~0	
$[Mo^{V}(^{3,5}L_{S,S})_3]^{-}$	$^1/_2$	1.00[b]	−0.09	

[a] Values in brackets are from ref 7 (spin-unrestricted BP calculations). [b] Spin-unrestricted B3LYP calculations. [c] BS B(3,3) calculation (B3LYP). [d] BS B(3,2) calculation (B3LYP). [e] BS B(3,1) calculation (B3LYP). [f] BS(3,3) calculation using the BP86 functional. [g] Coupling constant according to the Hamiltonian $\hat{H} = -2J\hat{S}_{rad}\cdot\hat{S}_{Cr(III)}$.

the quartet state of the trianion $[Cr(L_{cat})]^{3-}$ revealed in both instances the presence of three singly occupied orbitals (t_{2g}) (SOMOs), each of which possesses ~92% metal d character and only 7−8% ligand character. Thus, the trianion is a typical, distorted octahedral chromium(III) complex. The calculated Mulliken spin density (Table 6) shows the presence of three unpaired electrons at the central metal ion and none on the three closed-shell catecholate(2−) ligands. Exactly the same situation is encountered for the sulfur analogue $[Cr^{III}(^{3,5}L_{S,S})_3]^{3-}$ where again the three SOMOs have 92% metal 3d character and the Mulliken spin density of 3.2 is located at the chromium ion. No significant spin density was found on the ligands (an average of −0.05 on each sulfur atom).

The Monoanions. The electronic structure of the doublet state of $[Mo^{V}(^{3,5}L_{S,S})_3]^{-}$ shows a single SOMO with 73% Mo 4d character, a spin density of 1.0 at the central molybdenum(V) (d^1) ion, and virtually none on the ligands. This is the hallmark of a genuine Mo(V) ion in a nearly octahedral ligand field. The situation is now quite different for the doublet states of the two corresponding monoanions $[Cr^{III}(L^{\bullet}_{sq})_2(L_{cat})]^{-}$ and $[Cr^{III}(^{3,5}L^{\bullet}_{S,S})_2(^{3,5}L_{S,S})]^{-}$.

Figure 10 shows qualitative MO diagrams for the above two chromium complexes from spin-unrestricted BS(3,2) $M_S = {}^1/_2$ calculations at the B3LYP level. These calculations lead to BS(3,2) $M_S = {}^1/_2$ states which are lower in energy than the corresponding high-spin $S = {}^5/_2$ states. It is interesting to note that attempts to calculate a BS(4,3) or a BS(2,1) $M_S = {}^1/_2$ state converged back to the BS(3,2) solutions. Thus, electronic structure descriptions such as $[Cr^{II}(L^{\bullet}_{sq})_3]^{-}$/$[Cr^{II}(^{3,5}L^{\bullet}_{S,S})_3]^{-}$ or $[Cr^{IV}(L^{\bullet}_{sq})(L_{cat})_2]^{-}$/$[Cr^{IV}(^{3,5}L^{\bullet}_{S,S})(^{3,5}L_{S,S})_2]^{-}$ can safely be ruled out.

Three predominantly metal d orbitals are identified in $[Cr(L_{O,O})_3]^{-}$; they are Cr-based orbitals originating from the t_{2g} set (in O_h symmetry) and occur only in the spin-up manifold. These three orbitals are singly occupied with parallel spins. This orbital occupation pattern defines a Cr(III) configuration ($S_{Cr} = {}^3/_2$) at the metal center as in the above trianions. In addition to these three metal-centered orbitals, *two* ligand-centered orbitals are identified in the spin-down manifold which are not populated in the spin-up manifold, thus leading to the observed overall $M_S = {}^1/_2$ state.

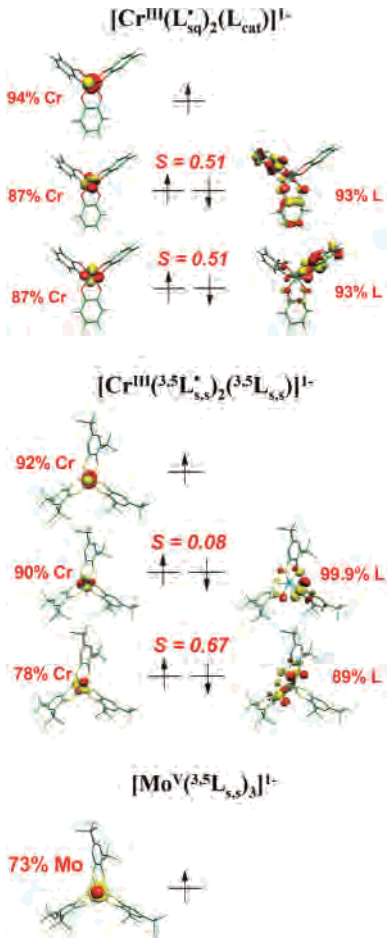

Figure 10. Qualitative MO diagrams for **[1]**$^{1-}$ (top), **[3]**$^{1-}$ (middle), and $[Mo^{V}(^{3,5}L_{S,S})_3]^{1-}$ (bottom) of the corresponding orbitals of magnetic pairs calculated at the B3LYP/TZV(P) level.

These orbitals correspond to two symmetry-adapted combinations of the SOMO of two ligand *o*-semiquinone radicals. Thus, the basic electronic structure description of both monoanions features a Cr(III) ion which is strongly antiferromagnetically coupled to two ligand-centered π radicals as has been traditionally proposed for $[Cr^{III}(L^{\bullet}_{sq})_2(L_{cat})]^{-}$. Our calculations do not support Lay et al.'s[7] description as $[Cr^{V}(L_{cat})_3]^{-}$. On the other hand, the $S = {}^1/_2$ calculation at the B3LYP level for $[Mo^{V}(L_{S,S})_3]^{-}$ clearly shows only a single metal d-centered SOMO; the three ligands are closed-shell dianions$(L_{S,S})^{2-}$ in agreement with an electronic structure description invoking a Mo(V) ion (d^1) and three closed-shell ligands.

In Figure 10 the corresponding orbital transformation[21] was used to visualize the overlapping magnetic pairs of the two systems. The spin orbitals obtained from single-point, unrestricted calculations were transformed in such a way that for each spin-up orbital there exists at most one spin-down partner that has nonzero spatial overlap. Values of S close to 1 indicate a standard doubly occupied MO with little spin-polarization, whereas $S \ll 1$ is the signature of non-orthogonal magnetic orbital pairs. For $[Cr^{III}(L^{\bullet}_{sq})_2(L_{cat})]^{-}$ and $[Cr^{III}(^{3,5}L^{\bullet}_{S,S})_2(^{3,5}L_{S,S})]^{-}$, two such magnetically interacting pairs (via a π pathway) have been identified. Each of these pairs consists of one metal orbital and the corresponding

ligand radical orbital. The mutual overlap between these two orbitals are 0.51 and 0.51 for $[\mathbf{1}]^{1-}$ and 0.08 and 0.67 for $[\mathbf{3}]^{1-}$.

In order to determine the exchange coupling constants, we examined the high-spin and BS energies together with the corresponding spin-expectation values $<\mathbf{S}^2>$ according to the Yamaguchi approach, eqs 7 and 8. The meaning of $<\mathbf{S}^2>$ has been described in ref 41.

$$H_{\mathrm{HDvV}} = -2J\hat{\mathbf{S}}_{\mathrm{A}}\cdot\hat{\mathbf{S}}_{\mathrm{B}} \tag{7}$$

$$J = \frac{E_{\mathrm{HS}} - E_{\mathrm{BS}}}{<\mathbf{S}^2>_{\mathrm{HS}} - <\mathbf{S}^2>_{\mathrm{BS}}} \tag{8}$$

The value estimated in this fashion for $[\mathbf{1}]^{1-}$ is -606 cm^{-1} and -714 cm^{-1} for $[\mathbf{3}]^{1-}$. This calculated large value is in good agreement with the experimental observation that both complexes possess a doublet ground state up to room temperature with no indication of thermal population of higher spin states. J is too large to be verified experimentally; the accuracy of the calculations cannot be assessed.

As pointed out previously,[42] the spin density arising from BS SCF (DF or HF) calculations is unphysical. Nevertheless, it is quite suggestive of the physical situation at hand. The spin density plots in Figure 11 for $[\mathbf{1}]^{1-}$, $[\mathbf{3}]^{1-}$, and $[\mathrm{Mo^V}(^{3,5}\mathrm{L}_{\mathrm{S,S}})_3]^{1-}$ nicely show the antiparallel spin alignment between the Cr(III) (positive spin density in red) and the radical ligands (negative spin density in yellow) and the fact that the molybdenum complex does not have a π-radical ligand. The approximate breakdown of the spin density into atomic contributions via spin population analyses (Table 6) supports the presence of the three unpaired electrons at the Cr ion (positive spin) and two unpaired electrons with a negative spin distributed over three ligands and a single unpaired electron of the $\mathrm{Mo^V}$ center. In contrast, the same analysis reported in ref 7 and our own BP86 calculations exhibit only ~2 unpaired electrons on the Cr ion (Cr(IV)?) and only one unpaired electron distributed over the three ligands. This would favor a description as $[\mathrm{Cr^{IV}}(\mathrm{L^{\bullet}_{sq}})(\mathrm{L_{cat}})_2]^{-}$ and not $[\mathrm{Cr^{V}}(\mathrm{L_{cat}})_3]^{-}$ as in ref 7 or $[\mathrm{Cr^{III}}(\mathrm{L^{\bullet}_{sq}})_2(\mathrm{L_{cat}})]^{1-}$ as we propose here.

The Dianions. Exactly the same analyses as described above for the monoanions were performed for the dianions $[\mathbf{1}]^{2-}$ and $[\mathbf{3}]^{2-}$ with triplet ground states. In both cases, BS-(3,1) solutions were found to be lower in energy than the corresponding high-spin $S = 2$ solutions.

In both cases, three singly occupied metal d orbitals indicative of a chromium(III) ion and one antiferromagnetically coupled ligand orbital containing one unpaired electron were identified; as shown in Figure S1 for $[\mathrm{Cr^{III}}(\mathrm{L^{\bullet}_{sq}})_2(\mathrm{L_{cat}})]^{2-}$, the corresponding MO scheme for $[\mathbf{3}]^{2-}$ is very similar. The

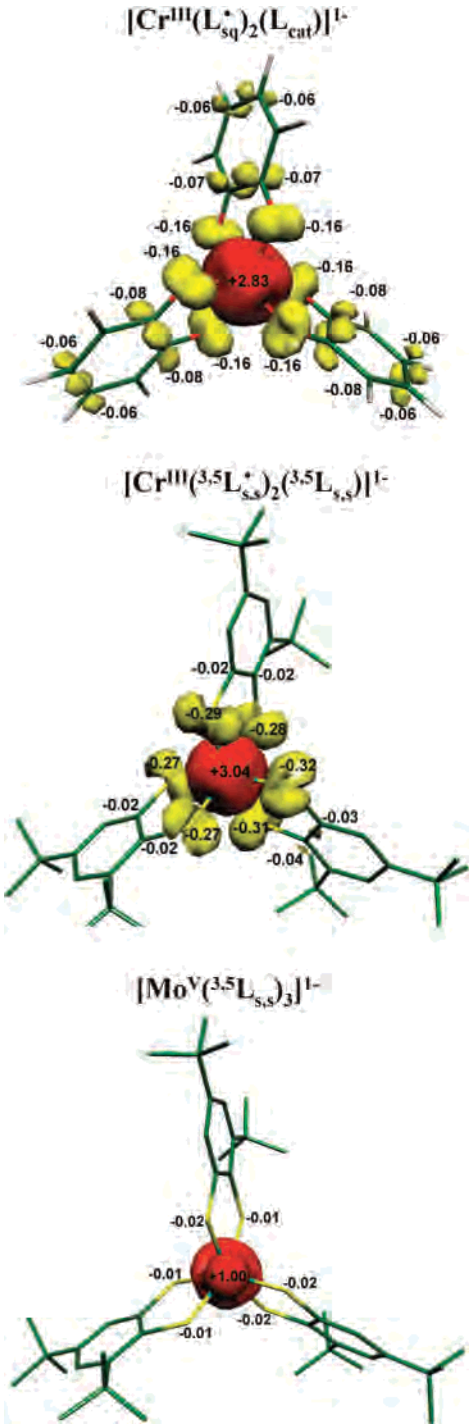

Figure 11. Spin density plots of $[\mathbf{1}]^{1-}$ (top), $[\mathbf{3}]^{1-}$ (middle), and $[\mathrm{Mo^V}(^{3,5}\mathrm{L}_{\mathrm{S,S}})_3]^{-}$ (bottom) as derived from BS DFT calculations together with values of the spin density of the Mulliken spin population analyses.

spin density analysis for $[\mathbf{1}]^{2-}$ and $[\mathbf{3}]^{2-}$ (Table 6) shows three unpaired electrons at the Cr metal atom and ~2 unpaired electrons distributed over three ligands. The electronic structure of the dianions are therefore best described as $[\mathrm{Cr^{III}}(\mathrm{L^{\bullet}_{sq}})(\mathrm{L_{cat}})_2]^{2-}$ and $[\mathrm{Cr^{III}}(^{3,5}\mathrm{L^{\bullet}_{S,S}})(^{3,5}\mathrm{L}_{\mathrm{S,S}})_2]^{2-}$ where the ligand-mixed valency is of class III (delocalized).

It is again significant that Lay et al.'s calculation[7] using the BP86 functional (spin-unrestricted $S = 1$) does not agree with our BS(3,1) B3LYP calculations.

(41) (a) Soda, T.; Kitagawa, Y.; Onishi, T.; Takano, Y.; Shigetu, Y.; Nagao, H.; Yoshioka, Y.; Yamaguchi, K. *Chem. Phys. Lett.* **2000**, *319*, 223. (b) Yamaguchi, K.; Takahara, Y.; Fueno, T. In *Applied Quantum Chemistry*; Smith, V. H., Ed.; Reidel: Dordrecht, The Netherlands, 1986; p 155.

(42) (a) Kirchner, B.; Wennmohs, F.; Ye, S.; Neese, F. *Curr. Opin. Chem. Biol.* **2007**, *11*, 134. (b) Neese, F. *J. Biol. Inorg. Chem.* **2006**, *11*, 702.

The Neutral Complexes. The electronic structure of the neutral complex $[Cr(L^{\bullet}_{sq})_3]^0$ has been calculated by using the BP86 and the B3LYP functional.

We found that the BS(3,3) solution for $[Cr(L^{\bullet}_{sq})_3]^0$ using the BP86 functional is ~10 kcal mol^{-1} *lower* in energy than the corresponding spin-unrestricted $S = 0$ calculation and also the corresponding high-spin state $S = 3$. The closed-shell spin-restricted $S = 0$ solution implying a $[Cr^{VI}(L_{cat})_3]^0$ electronic structure is found 50 kcal mol^{-1} higher in energy and is therefore not considered further. It is also important to note that attempts to generate a BS(2,2), BS(1,1), or a spin-unrestricted $S = 0$ solution by using the B3LYP functional failed; they converged back to the BS(3,3) solution, which is lower in energy as compared to the high-spin $S = 3$ solution by 12.7 kcal mol^{-1}.

A qualitative bonding scheme derived from the B3LYP BS $M_S = 0$ calculation of $[Cr^{III}(L^{\bullet}_{sq})_3]$ is shown in Figure S2. Three half-occupied orbitals of mainly chromium character (t_{2g} set) are identified; they are singly occupied with parallel (spin-up) spins. This orbital occupation pattern defines a (high-spin) chromium(III) configuration ($S_{Cr} = {}^3/_2$) at the metal center. In addition, three ligand-centered orbitals are identified in the spin-down manifold that are not populated in the spin-up manifold, thus leading to the observed overall $M_S = 0$ state. The basic electronic structure description features a Cr(III) ion ($S_{Cr} = {}^3/_2$) that is strongly antiferromagnetically coupled to three ligand-centered *o*-semiquinonate π radicals as has been proposed by all previous authors.[1−4]

The Mulliken spin-population analysis (Table 6) of $[Cr^{III}(L^{\bullet}_{sq})_3]$ is in perfect agreement with this notion. Three unpaired electrons (α-spins) are located at the chromium center, and three unpaired electrons are located in three π ligand orbitals as shown in Figure S3. If the same spin-analysis is performed for the BS(3,3) $M_S = 0$ solution using the BP86 functional, the overall bonding picture remains the same, but the spin densities are significantly smaller (−2.2 unpaired electrons at the chromium ion and 2.2 unpaired electrons on the three ligands).

It is very instructive to break down the ligand spin density to their corresponding atomic contributions. The spin density of a given *o*-semiquinonate(1−) π-radical ligand is distributed 46% on the two oxygen atoms and 54% in the six-membered carbon ring. Very similar results have been obtained for $[Cr^{III}(^{3,5}L^{\bullet}_{S,S})_3]$, as shown in Figures S2 and S3. Again, a central Cr(III) ion ($S_{Cr} = {}^3/_2$) is identified, as well as three antiferromagnetically coupled π-radical ligands $(^{3,5}L^{\bullet}_{S,S})^{1-}$. The Mulliken spin population analysis reveals the presence of 3.03 unpaired electrons at the metal ion (α-spins) and 2.8 unpaired electrons on the three ligands (β-spins). Note that the ligand spin population is ~78% on the sulfur atoms and very little (15%) on the six-membered C-ring. This is typical for organic S-centered radicals.[26,34c] Thus, the electronic structure is best described as $[Cr^{III}(^{3,5}L^{\bullet}_{S,S})_3]^0$.

Conclusions

We have shown in this study that the well-known tris(dioxolene)chromium complexes consisting of a neutral, a mono-, di-, and trianionic species and forming an electron-transfer series has its sulfur containing analogue $[Cr(^{3,5}L_{S,S})_3]^z$ ($z = 0, 1-, 2-, 3-$).[32b] The electronic structures of the members of both series have been determined by UV−vis and IR spectroscopy, S and Cr K-edge XAS, X-ray crystallography, and most significantly, by BS DFT calculations by using the B3LYP/TZV(P) functional. The following results have been obtained.

(1) The electronic structures of the trianions $[Cr^{III}(^{3,6}L_{cat})_3]^{3-}$ and $[Cr^{III}(^{3,5}L_{S,S})_3]^{3-}$ are best described as classic distorted octahedral chromium(III) (d^3; $S_t = {}^3/_2$) species containing three closed-shell, bidentate catecholate(2−) and three closed-shell 3,5-di-*tert*-butylbenzene-1,2-dithiolate(2−) ligands, respectively. Spin-unrestricted $S = {}^3/_2$ DFT calculations (BP86[7] and B3LYP) are in excellent agreement with this notion: the HOMO, HOMO-1, and HOMO-2 orbitals are each half-filled, yielding an overall Mulliken spin density of 3.0. They possess >90% metal d character. Both UV−vis spectra display two weak d−d transitions in the visible, as is expected for an octahedral Cr(III) complex. This interpretation of the electronic structure of [**1**]$^{3-}$ is in agreement with all previous studies.[1−7]

(2) The electronic structure description of the neutral complex $[Cr^{III}(^{3,6}L_{sq})_3]$ as containing three *o*-semiquinonate(1−) ligand π radicals ($S_{rad} = {}^1/_2$) and an intramolecularly, antiferromagnetically coupled central chromium(III) ion ($S_{Cr} = {}^3/_2$) generating the overall diamagnetic ground state ($S = 0$) has been predominantly based on the experimental crystal structure by all previous authors and us here. Three O,O′-coordinated *o*-semiquinonates(1−) have been identified by their relatively short C−O bonds and the clear quinoid-type distortion of the six-membered carbon rings (two alternating short C=C bonds and four longer C−C single bonds). It is therefore an important result that the BS(3,3) DFT calculations using the B3LYP or BP86 functional are lower in energy than the spin-unrestricted $S = 0$ solutions by 10 kcal mol^{-1}. Mulliken spin population analysis of the calculated BS(3,3) B3LYP electronic structure reveals the presence of three unpaired electrons (α-spins) at the chromium(III) and three unpaired electrons on the *o*-semiquinonate radicals (β-spins). The same analysis for the BP86 solution yields a spin density of only 2.2 electrons at the Cr center and only 2.2 on the three ligands proving that the BP86 functional is not adequate for describing the electronic structure of this complex.

The electronic spectrum of the electrochemically generated neutral complex $[Cr^{III}(^{3,5}L^{\bullet}_{S,S})_3]^0$ is very similar to that of the above tris(*o*-semiquinonato)chromium(III) derivative. The BS(3,3) DFT calculations again show the presence of a central Cr(III) ion (d^3) and three π-radical monoanions which couple antiferromagnetically with the three unpaired electrons of the Cr(III) center, yielding a diamagnetic ground state.

(3) The electronic structure of the paramagnetic monoanion $[Cr(L_{O,O})_3]^-$ is discussed controversially as $[Cr^{III}(L^{\bullet}_{sq})_2(L_{cat})]^-$

($S = {}^1/_2$) or as $[Cr^V(L_{cat})_3]^-$. It is therefore an important observation that the XAS Cr K-edge and pre-edge energies of the neutral species $[Cr^{III}(L^{\bullet}_{sq})_3]^0$ and of the monoanion are *identical. This is a clear indication that the oxidation state of the central chromium ion in both species is the same, namely +III ($S_{Cr} = {}^3/_2$).* BS(3,2) DFT calculations (B3LYP) nicely corroborate this notion because there are three unpaired electrons at the Cr(III) ion (α-spin) and two unpaired electrons distributed over three ligands (β-spin). These results are in conflict with Lay et al.'s[7] $S = {}^1/_2$ DFT calculations using the BP86 functional. Further spectroscopic evidence for the class III (delocalized) ligand mixed valency in the monoanion is deduced from the presence of an intense IVCT band at 1700 nm ($\epsilon = 8000\ M^{-1}\ cm^{-1}$). This band is absent in the electronic spectrum of **1** and $[\mathbf{1}]^{3-}$.

The electronic spectrum of the sulfur analogue $[Cr(^{3,5}L_{S,S})_3]^-$ is very similar to that of $[Cr^{III}(^{3,6}L^{\bullet}_{sq})_2(^{3,6}L_{cat})]^-$: the IVCT band is observed at 1750 nm ($\epsilon = 3000\ M^{-1}\ cm^{-1}$). The XAS Cr K-edge and pre-edge energies of $[\mathbf{3}]^-$ are at lower energies than in $[\mathbf{1}]^-$ by ~0.9 eV, which is due to the presence of six softer sulfur donor atoms in $[\mathbf{3}]^-$ with an increased Cr−S covalency as compared to the six Cr−O bonds in $[\mathbf{1}]^-$. Most significantly, the XAS S K-edge spectra of isostructural $[N(n\text{-}Bu)_4][M(^{3,5}L_{S,S})_3]$ (M = Cr, Mo) are different. The spectrum of $[\mathbf{3}]^-$ reveals the presence of π-radical ligands $(^{3,5}L^{\bullet}_{S,S})^{1-}$ which are absent in $[Mo^V(^{3,5}L_{S,S})_3]^-$. The present experimental data and the DFT calculations corroborate electronic structure descriptions as $[Cr^{III}(^{3,5}L^{\bullet}_{S,S})_2(^{3,5}L_{S,S})]^-$ and $[Mo^V(^{3,5}L_{S,S})_3]^-$.

(4) The electronic structures of the two dianions $[\mathbf{1}]^{2-}$ ($S = 1$) and $[\mathbf{3}]^{2-}$ ($S = 1$) are again very similar. Their electronic spectra are nearly identical in character, and both display intense ligand mixed valency IVCT bands in the NIR, indicating that both ions possess one ligand π radical, namely $(^{3,6}L^{\bullet}_{sq})^{1-}$ and $(^{3,5}L^{\bullet}_{S,S})^{1-}$, respectively. The BS(3,1) DFT calculations using the B3LYP functional show that both dianions possess three unpaired electrons in metal d orbitals (Cr^{III}; d^3) and one unpaired electron distributed over three ligands (class III; delocalized). Intramolecular antiferromagnetic coupling affords the $S = 1$ ground states.

In summary, we have provided here consistent and compelling evidence that the redox processes in the two electron-transfer series of $[Cr(^{3,6}L_{O,O})_3]^z$ and $[Cr(^{3,5}L_{S,S})_3]^z$ ($z = 0, 1-, 2-, 3-$) are purely ligand-based. We have not found evidence for the occurrence of Cr(IV) and Cr(V) ions in any of these complexes.

Acknowledgment. We thank Prof. F. Neese (Universität Bonn) for his help with the calculations and his interest in the problem. We are grateful for financial support from the Fonds der Chemischen Industrie. R.R.K. and N.M. thank the Max-Planck-Society for doctoral and postdoctoral stipends, respectively. SSRL operations are funded by the Department of Energy, Office of Basic Energy Sciences. The Structural Molecular Biology program is supported by the National Institutes of Health, National Center of Research Resources, Biomedical Technology Program and by the Department of Energy, Office of Biological and Environmental Research.

Supporting Information Available: X-ray crystallographic files in CIF format for **1** and **3** and tables of geometrical and electronic structural details of BS DFT calculated structures. Figures S1 and S2 show qualitative MO diagrams for $[\mathbf{1}]^{2-}$ and the neutral complexes $[\mathbf{1}]^0$ and $[\mathbf{3}]^0$, respectively. Figure S3 displays spin density plots of $[1]^0$ and $[3]^0$. This material is available free of charge via the Internet at http://pubs.acs.org.

IC7008607